

# Syntheses and structural characterization of heterometallic bis(pyrazolyl)methane complexes of rhenium and platinum

Daniel L. Reger <sup>\*</sup>, Russell P. Watson, Mark D. Smith

*Department of Chemistry and Biochemistry, University of South Carolina, Columbia, SC 29208, USA*

Received 2 August 2007; received in revised form 23 August 2007; accepted 23 August 2007

Available online 29 August 2007

## Abstract

The new heterometallic complex  $\{\mu\text{-}1,3,5\text{-}[\text{CH}(\text{pz})_2]_3\text{C}_6\text{H}_3\}\text{[Re}(\text{CO})_3\text{Br}]\text{[Pt}(p\text{-tolyl})_2]_2$  has been prepared by reaction of 1 equiv. of the dimer  $[\text{Pt}(p\text{-tolyl})_2(\mu\text{-SEt}_2)]_2$  with the monometallic rhenium precursor  $\{1,3,5\text{-}[\text{CH}(\text{pz})_2]_3\text{C}_6\text{H}_3\}\text{Re}(\text{CO})_3\text{Br}$ , where  $1,3,5\text{-}[\text{CH}(\text{pz})_2]_3\text{C}_6\text{H}_3$  is the tritopic, arene-linked bis(pyrazolyl)methane ligand 1,3,5-tris[bis(1-pyrazolyl)methyl]benzene. Similarly, the heterometallic complex  $\{\mu\text{-}1,3,5\text{-}[\text{CH}(\text{pz})_2]_3\text{C}_6\text{H}_3\}\text{[Re}(\text{CO})_3\text{Br}]\text{[Pt}(p\text{-tolyl})_2]$  has been made by the reaction of the dirhenium compound  $\{\mu\text{-}1,3,5\text{-}[\text{CH}(\text{pz})_2]_3\text{C}_6\text{H}_3\}\text{[Re}(\text{CO})_3\text{Br}]_2$  and one-half of an equivalent of  $[\text{Pt}(p\text{-tolyl})_2(\mu\text{-SEt}_2)]_2$ . X-ray crystallographic studies of the new compounds reveal significant noncovalent interactions in their molecular and supramolecular structures.

© 2007 Elsevier B.V. All rights reserved.

**Keywords:** Bis(pyrazolyl)methane; Tricarbonylrhenium(I); Ditolylplatinum(II); Supramolecular

## 1. Introduction

We previously reported the direct synthesis of the heterobimetallic complex  $\{\mu\text{-}m\text{-}[\text{CH}(\text{pz})_2]_2\text{C}_6\text{H}_4\}\text{[Re}(\text{CO})_3\text{Br}]\text{[Pt}(p\text{-tolyl})_2]$  by the addition of a tricarbonylrhenium(I) fragment to the bitopic, bis(pyrazolyl)methane ligand,  $m\text{-}[\text{CH}(\text{pz})_2]_2\text{C}_6\text{H}_4$ , to give the monometallic intermediate  $\{m\text{-}[\text{CH}(\text{pz})_2]_2\text{C}_6\text{H}_4\}\text{Re}(\text{CO})_3\text{Br}$ , followed by the addition of the ditolylplatinum center [1]. This heterometallic complex is the first to have been isolated with this class of symmetrical third-generation bis(pyrazolyl)methane compounds, where two or more bis(pyrazolyl)methyl groups are linked through organic spacers of varying flexibilities to produce polytopic ligands capable of forming multimetallic complexes [2]. Thus, we achieved the frequently unfeasible, selective formation [3] of a monometallic intermediate containing a ligating site available for subsequent coordination to a second metal fragment type.

This successful synthesis using a bitopic ligand and the propensity for heterometallic complexes to show unique

reactivity and catalytic applications compared to their homometallic analogues [4], prompted us to investigate a series of multimetallic complexes that could potentially be made using a symmetric, tritopic ligand linked by an aromatic group. The related tritopic compound  $1,3,5\text{-}(\text{CH}_3)_3\text{C}_6[\text{CH}_2\text{OCH}_2\text{C}(\text{pz})_3]_3$ , containing tridentate tris(pyrazolyl)methyl groups bound through aliphatic ether groups to a mesitylene ring, had already been prepared [5], and this ligand was termed “semi-rigid” considering the flexibility of the ether linkages and the rigidity of the arene ring. We wished to prepare heterometallic complexes with more fixed ligands so as to gain more control over the orientation of the metal centers. Based on our experience, however, with the low solubility of a more rigid (“fixed”) ligand in which tridentate heteroscorpionate groups were substituted directly onto the arene ring [6], we reasoned that the fixed, bidentate bis(pyrazolyl)methane compound would be more useful.

Accordingly, we prepared the tritopic bis(pyrazolyl)methane ligand  $1,3,5\text{-}[\text{CH}(\text{pz})_2]_3\text{C}_6\text{H}_3$  and demonstrated that it was possible to selectively add one, two, or three  $[\text{Re}(\text{CO})_3\text{Br}]$  units to yield the mono-, bi-, and trimetallic complexes  $\{1,3,5\text{-}[\text{CH}(\text{pz})_2]_3\text{C}_6\text{H}_3\}\text{Re}(\text{CO})_3\text{Br}$ ,

<sup>\*</sup> Corresponding author. Fax: +1 803 777 9521.

E-mail address: [reger@mail.chem.sc.edu](mailto:reger@mail.chem.sc.edu) (D.L. Reger).

{ $\mu$ -1,3,5-[CH(pz)<sub>2</sub>]<sub>3</sub>C<sub>6</sub>H<sub>3</sub>}[Re(CO)<sub>3</sub>Br]<sub>2</sub>, and { $\mu$ -1,3,5-[CH(pz)<sub>2</sub>]<sub>3</sub>C<sub>6</sub>H<sub>3</sub>}[Re(CO)<sub>3</sub>Br]<sub>3</sub> [7]. Herein, we report the use of the mono- and dirhenium complexes to prepare the heterometallic compounds { $\mu$ -1,3,5-[CH(pz)<sub>2</sub>]<sub>3</sub>C<sub>6</sub>H<sub>3</sub>}[Re(CO)<sub>3</sub>Br][Pt(*p*-tolyl)<sub>2</sub>]<sub>2</sub> (**1**) and { $\mu$ -1,3,5-[CH(pz)<sub>2</sub>]<sub>3</sub>C<sub>6</sub>H<sub>3</sub>}-[Re(CO)<sub>3</sub>Br]<sub>2</sub>[Pt(*p*-tolyl)<sub>2</sub>]<sub>2</sub> (**2**). The solid state molecular and supramolecular structures of these heterometallic complexes are also presented.

## 2. Experimental

### 2.1. General considerations

Air-sensitive materials were handled under a nitrogen atmosphere using standard Schlenk techniques. All solvents were dried and distilled by conventional methods prior to use. The compounds {1,3,5-[CH(pz)<sub>2</sub>]<sub>3</sub>C<sub>6</sub>H<sub>3</sub>}Re(CO)<sub>3</sub>Br [7], { $\mu$ -1,3,5-[CH(pz)<sub>2</sub>]<sub>3</sub>C<sub>6</sub>H<sub>3</sub>}[Re(CO)<sub>3</sub>Br]<sub>2</sub> [7], and [Pt(*p*-tolyl)<sub>2</sub>( $\mu$ -SEt<sub>2</sub>)]<sub>2</sub> [8] were prepared as previously described. All other chemicals were purchased from Aldrich or Fisher Scientific and used as received. Reported melting points are uncorrected. IR spectra were obtained on a Nicolet 5DXBO FTIR spectrometer. <sup>1</sup>H NMR spectra were recorded on a Mercury/VX 300 or Mercury/VX 400 spectrometer. All chemical shifts are in ppm and are secondary-referenced using the signals from residual undeuterated solvents. Mass spectrometric measurements were obtained on a MicroMass QTOF spectrometer. Elemental analyses were performed on vacuum-dried samples by Robertson Microlit Laboratories (Madison, NJ).

### 2.2. Syntheses

#### 2.2.1. { $\mu$ -1,3,5-[CH(pz)<sub>2</sub>]<sub>3</sub>C<sub>6</sub>H<sub>3</sub>}[Re(CO)<sub>3</sub>Br]-[Pt(*p*-tolyl)<sub>2</sub>]<sub>2</sub> (**1**)

{1,3,5-[CH(pz)<sub>2</sub>]<sub>3</sub>C<sub>6</sub>H<sub>3</sub>} Re(CO)<sub>3</sub>Br (0.10 g, 0.12 mmol) and [Pt(*p*-tolyl)<sub>2</sub>( $\mu$ -SEt<sub>2</sub>)]<sub>2</sub> (0.12 g, 0.13 mmol) were dissolved in 15 mL of CH<sub>2</sub>Cl<sub>2</sub> and stirred at room temperature for 24 h. The solvent was removed by rotary evaporation and the resulting solid recrystallized by the vapor diffusion of diethyl ether into acetone solutions of the product. Crystals for X-ray studies were taken directly from the mother liquor. Crystals for all other characterization were removed, rinsed with diethyl ether, and dried *in vacuo*, resulting in loss of the solvent of crystallization. M.p.: 184 °C dec. Anal. Calc. for C<sub>58</sub>H<sub>52</sub>BrN<sub>12</sub>O<sub>3</sub>Pt<sub>2</sub>Re: C, 42.97; H, 3.23; N, 10.37. Found: C, 43.14; H, 2.92; N, 10.19%. IR,  $\nu_{\text{CO}}$  (KBr, cm<sup>-1</sup>): 2025, 1925, 1882. <sup>1</sup>H NMR (300 MHz, acetone-*d*<sub>6</sub>):  $\delta$  8.83 (s, 1H, CH(pz)<sub>2</sub>[Re]), 8.38 (s, 2H, CH(pz)<sub>2</sub>[Pt]), 8.22, 7.31 (br s, d, *J* = 1.8 Hz; 4 H, 4H, 3,5-H pz[Pt]), 8.11, 7.89 (d, *J* = 1.8 Hz, br s; 2H, 2 H, 3,5-H pz[Re]), 6.94 (d, *J* = 8.1 Hz, *J*<sub>PtH</sub> = 54 Hz, 8H, 2,6-C<sub>6</sub>H<sub>4</sub>CH<sub>3</sub>), 6.65 (d, *J* = 7.2 Hz, 8H, 3,5-C<sub>6</sub>H<sub>4</sub>CH<sub>3</sub>), 6.37 (t, *J* = 2.6 Hz, 4H, 4-H pz[Pt]), 6.32 (t, *J* = 2.6 Hz, 2H, 4-H pz[Re]), 5.52 (br s, 2H, C<sub>6</sub>H<sub>3</sub>), 5.01 (br s, 1H, C<sub>6</sub>H<sub>3</sub>), 2.12 (s, 12H, C<sub>6</sub>H<sub>4</sub>CH<sub>3</sub>). MS: ESI(+) *m/z* (Rel. Int.%) [assgn]: 1660 (70) [M + K]<sup>+</sup>, 1622 (15) [M + H]<sup>+</sup>.

HRMS: ESI(+) (*m/z*) Calc. for C<sub>58</sub>H<sub>52</sub>BrN<sub>12</sub>NaO<sub>3</sub>Pt<sub>2</sub>Re, [M + Na]<sup>+</sup>, 1644.2209; found 1644.2207.

#### 2.2.2. { $\mu$ -1,3,5-[CH(pz)<sub>2</sub>]<sub>3</sub>C<sub>6</sub>H<sub>3</sub>}[Re(CO)<sub>3</sub>Br]<sub>2</sub>-[Pt(*p*-tolyl)<sub>2</sub>]<sub>2</sub> (**2**)

A suspension of { $\mu$ -1,3,5-[CH(pz)<sub>2</sub>]<sub>3</sub>C<sub>6</sub>H<sub>3</sub>}[Re(CO)<sub>3</sub>Br]<sub>2</sub> (0.10 g, 0.082 mmol) and [Pt(*p*-tolyl)<sub>2</sub>( $\mu$ -SEt<sub>2</sub>)]<sub>2</sub> (0.040 g, 0.043 mmol) in 20 mL of CH<sub>2</sub>Cl<sub>2</sub> was stirred at room temperature for 2 d. The white product was isolated by gravity filtration, washed with 5 mL of CH<sub>2</sub>Cl<sub>2</sub> and dried *in vacuo*. Yield = 0.064 g (49%). M.p.: >300 °C. IR,  $\nu_{\text{CO}}$  (KBr, cm<sup>-1</sup>): 2026, 1924, 1892. <sup>1</sup>H NMR (400 MHz, acetone-*d*<sub>6</sub>):  $\delta$  8.60 (s, 2H, CH(pz)<sub>2</sub>[Re]), 8.33, 7.39 (br s, br s; 2H, 2H, 3,5-H pz[Pt]), 8.26 (s, 1H, CH(pz)<sub>2</sub>[Pt]), 8.09, 8.06 (d, *J* = 2.0 Hz, br s; 4H, 4H, 3,5-H pz[Re]), 6.96 (d, *J* = 7.6 Hz, *J*<sub>PtH</sub> = 72 Hz, 4H, 2,6-C<sub>6</sub>H<sub>4</sub>CH<sub>3</sub>), 6.67 (d, *J* = 7.6 Hz, 4 H, 3,5-C<sub>6</sub>H<sub>4</sub>CH<sub>3</sub>), 6.56 (t, *J* = 2.6 Hz, 4H, 4-H pz[Re]), 6.49 (t, *J* = 2.6 Hz, 2H, 4-H pz[Pt]), 5.96 (br s, 2H, C<sub>6</sub>H<sub>3</sub>), 5.91 (br s, 1H, C<sub>6</sub>H<sub>3</sub>), 2.08 (s, 6H, C<sub>6</sub>H<sub>4</sub>CH<sub>3</sub>). MS: ESI(+) *m/z* (Rel. Int.%) [assgn]: 1612 (80) [M + NH<sub>4</sub>]<sup>+</sup>, 1595 (50) [M + H]<sup>+</sup>, 1503 (100) [M - C<sub>6</sub>H<sub>4</sub>CH<sub>3</sub>]<sup>+</sup>, 1487 (60) [M - Br - CO]<sup>+</sup>. Crystals for X-ray studies were grown by the vapor diffusion of diethyl ether in acetonitrile solutions of the solid and were taken directly from the mother liquor.

### 2.3. X-ray crystallographic analyses

Details of the data collections for **1** and **2** · CH<sub>3</sub>CN are given in Table 1. X-ray diffraction intensity data for **2** · CH<sub>3</sub>CN were measured at 150(1) K on a Bruker SMART APEX diffractometer (Mo K $\alpha$  radiation,  $\lambda$  = 0.71073 Å) [9]. Crystals of **1** suffered rapid (within a few seconds) clouding and loss of crystallinity when removed from the mother liquor, even under paratone-N oil. Despite repeated efforts a successful transfer of an intact crystal of **1** to the cold stream for a low-temperature data collection could not be achieved before decomposition. The crystals are stable indefinitely in the acetone/ether growth solvent mixture, and therefore the data collection was carried out using a crystal mounted in the mother liquor inside a thin-walled capillary tube sealed on both ends with putty and epoxy. The X-ray intensity data for **1** were measured at 294(1) K on the same Bruker diffractometer as above. Raw area detector data frame integration was performed with SAINT+ [9]. Both data sets were corrected for absorption effects with SADABS [9]. Direct or Patterson methods structure solution, difference Fourier calculations, and full-matrix least-squares refinement against *F*<sup>2</sup> were performed with SHELXTL [10]. Important notes regarding the solution and refinement for both structures follow.

Complex **1** refined normally with the exception of one of the two -C<sub>6</sub>H<sub>4</sub>CH<sub>3</sub> substituents bound to Pt(2). This group (C(111)–C(117)/C(211)–C(217)) is disordered equally over two orientations. The Pt(2)-bound carbon (C(111)/C(211)) was kept common to both disorder components,

Table 1

Crystal data and refinement details for  $\{\mu\text{-}1,3,5\text{-}[\text{CH}(\text{pz})_2]_3\text{C}_6\text{H}_3\}[\text{Re}(\text{CO})_3\text{Br}][\text{Pt}(p\text{-tolyl})_2]_2$  (**1**) and  $\{\mu\text{-}1,3,5\text{-}[\text{CH}(\text{pz})_2]_3\text{C}_6\text{H}_3\}[\text{Re}(\text{CO})_3\text{Br}]_2\text{-}[\text{Pt}(p\text{-tolyl})_2] \cdot \text{CH}_3\text{CN}$  (**2** ·  $\text{CH}_3\text{CN}$ )

	<b>1</b>	<b>2</b> · $\text{CH}_3\text{CN}$
Empirical formula	$\text{C}_{58}\text{H}_{52}\text{BrN}_{12}\text{O}_3\text{Pt}_2\text{Re}$	$\text{C}_{49}\text{H}_{41}\text{Br}_2\text{N}_{13}\text{O}_6\text{PtRe}_2$
Formula weight	1621.41	1635.26
Temperature (K)	294(1)	150(1)
Crystal system	Triclinic	Monoclinic
Space group	$P\bar{1}$	$P2_1/c$
Unit cell dimensions		
<i>a</i> (Å)	11.9947(17)	12.1586(5)
<i>b</i> (Å)	16.725(2)	25.7553(10)
<i>c</i> (Å)	21.646(3)	17.0329(7)
$\alpha$ (°)	106.909(3)	90
$\beta$ (°)	94.465(3)	102.5290(10)
$\gamma$ (°)	95.647(3)	90
<i>V</i> (Å <sup>3</sup> )	4108.6(10)	5206.8(4)
<i>Z</i>	2	4
<i>D</i> <sub>calc</sub> (Mg m <sup>-3</sup> )	1.311	2.086
Absorption coefficient (mm <sup>-1</sup> )	5.390	8.914
Absorption correction	Semi-empirical from equivalents	
<i>F</i> (000)	1548	3088
Crystal size (mm <sup>3</sup> )	0.46 × 0.24 × 0.18	0.30 × 0.12 × 0.06
$\theta$ Range for data collection (°)	1.72–24.16	1.46–26.39
Index ranges	–13 ≤ <i>h</i> ≤ 13, –19 ≤ <i>k</i> ≤ 19, –24 ≤ <i>l</i> ≤ 24	–15 ≤ <i>h</i> ≤ 15, –32 ≤ <i>k</i> ≤ 32, –21 ≤ <i>l</i> ≤ 21
Radiation, $\lambda$ (Å)	Mo K $\alpha$ , 0.71073	
Reflections collected	38677	58330
Independent reflections	13138	10657
Completeness to $\theta_{\text{max}}$ (%)	99.9	99.9
Final <i>R</i> indices [ <i>I</i> > 2 $\sigma$ ( <i>I</i> )]	$R_1 = 0.0338$ ; $wR_2 = 0.0841$	$R_1 = 0.0429$ ; $wR_2 = 0.1067$
Goodness-of-fit on <i>F</i> <sup>2</sup>	0.954	1.091

and the geometry of both was restrained to be similar to that of a normal tolyl group (C(81)–C(87)). Six independent solvent regions were located. The electron density features in three of these regions resembled acetone molecules; the remaining regions were featureless. All potential acetone molecules were apparently fractionally occupied over multiple orientations and were unstable toward refinement despite numerous modeling attempts. For this reason all disordered solvent was treated with the SQUEEZE option in PLATON [11]. The program calculated a solvent-accessible volume of 1561.2 Å<sup>3</sup> (37.3% of the total unit cell volume), corresponding to 155 electrons per cell. The contribution of these electrons was then removed from subsequent structure factor calculations. The reported FW, density, and *F*(000) reflect known unit cell contents only. The high solvent content and loosely bound (disordered) nature of these molecules explains the rapid decomposition (desolvation) of the crystals when removed from the mother liquor.

For compound **2** ·  $\text{CH}_3\text{CN}$  there is a single large (4.90 e<sup>-</sup>/Å<sup>3</sup>) residual electron density peak in the final difference map, located in a chemically impossible position (1.28 Å from H(1) and 1.49 Å from H(21)). The next largest peak is 2.96 e<sup>-</sup>/Å<sup>3</sup>, located <1 Å from Pt(1). The large peak persists despite trial application of different absorp-

tion correction methods. There is no evidence of twinning or degradation of the data crystal, and currently there is no explanation for this peak.

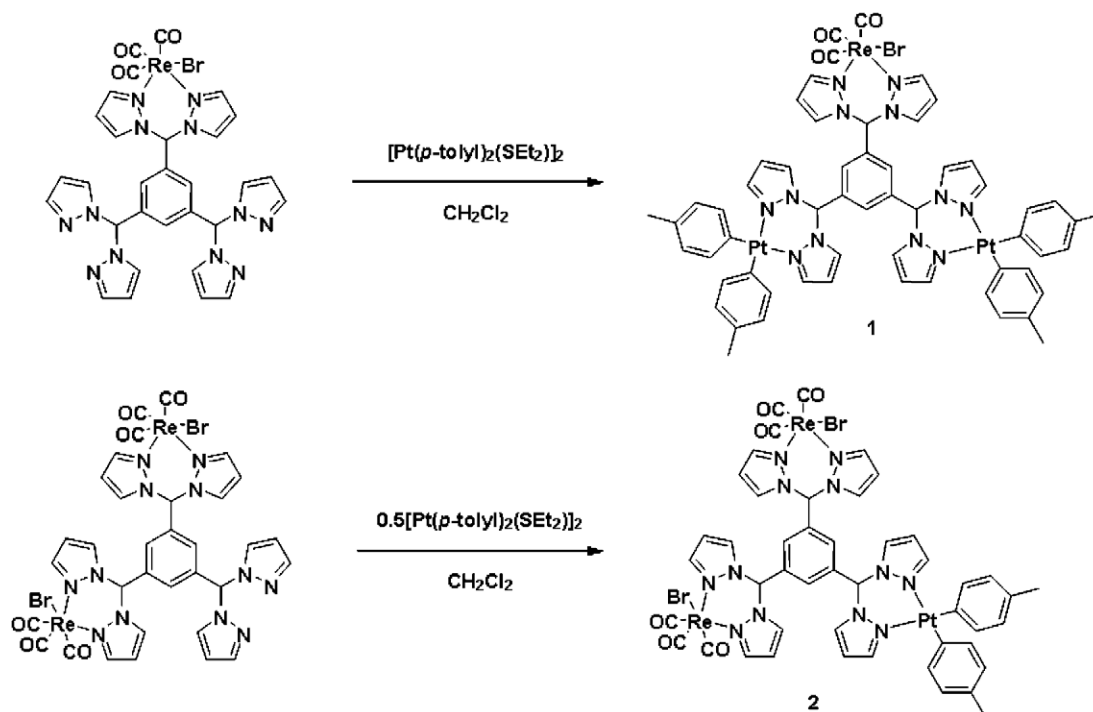
### 3. Results and discussion

#### 3.1. Syntheses

The monometallic rhenium complex 1,3,5- $[\text{CH}(\text{pz})_2]_3\text{-C}_6\text{H}_3\}[\text{Re}(\text{CO})_3\text{Br}]$  reacted with 1 equiv. of dimeric  $[\text{Pt}(p\text{-tolyl})_2(\mu\text{-SEt}_2)]_2$  in dichloromethane at room temperature to afford the heterometallic complex  $\{\mu\text{-}1,3,5\text{-}[\text{CH}(\text{pz})_2]_3\text{-C}_6\text{H}_3\}[\text{Re}(\text{CO})_3\text{Br}][\text{Pt}(p\text{-tolyl})_2]_2$  (**1**) in which two platinum(II) centers were incorporated into the uncoordinated ligating sites of the monorhenium precursor (Scheme 1). Similarly, one-half of an equivalent of  $[\text{Pt}(p\text{-tolyl})_2(\mu\text{-SEt}_2)]_2$  reacted with the dirhenium complex  $\{\mu\text{-}1,3,5\text{-}[\text{CH}(\text{pz})_2]_3\text{-C}_6\text{H}_3\}[\text{Re}(\text{CO})_3\text{Br}]_2$  to yield the compound  $\{\mu\text{-}1,3,5\text{-}[\text{CH}(\text{pz})_2]_3\text{-C}_6\text{H}_3\}[\text{Re}(\text{CO})_3\text{Br}]_2[\text{Pt}(p\text{-tolyl})_2]$  (**2**; Scheme 1), which contains one platinum(II) center.

The <sup>1</sup>H NMR spectra of **1** and **2** can be assigned based on the spectra of the mono- and dirhenium starting materials [7] and the relative integrations of the observed signals. That is, in **1** the ratio of signal integrations of the bis(pyrazolyl)methyl groups coordinated to the platinum centers to those pyrazolyl groups coordinated to the rhenium center is 2:1, and the same ratio in **2** is 1:2. For example, in **1** the methine proton associated with the rhenium center resonates at 8.83 ppm, whereas the methine protons associated with the platinum centers resonate at 8.38 ppm with double the integration of the former. Similarly, the 3/5-pyrazolyl protons on rings bound to rhenium are detected at 8.11 and 7.89 ppm, while signals from the analogous protons associated with platinum appear at 8.22 and 7.31 ppm and again integrate at twice the value as the rhenium-bound rings. The central aromatic ring in **1** contains two protons ortho to both rhenium- and platinum-bound bis(pyrazolyl)methyl substituents. These protons resonate at 5.52 ppm with twice the integration of the remaining resonance, which is between two platinum-associated bis(pyrazolyl)methyl groups and is detected upfield at 5.01 ppm. The tolyl groups bound to platinum are identified by resonances at 6.94, 6.65, and 2.12 ppm, with the expected <sup>195</sup>Pt-induced satellites around the signal at 6.94 ppm giving *J*<sub>PtH</sub> of 54 Hz. The <sup>1</sup>H NMR spectrum of **2** is completely analogous but with the already mentioned difference that the protons associated with rhenium coordination account for twice the signal integration of those protons on platinum-bound bis(pyrazolyl)methyl groups.

The positive ion electrospray mass spectrum of **1** shows peaks corresponding to the molecule associated with potassium cation and a proton at *m/z* of 1660 and 1622, respectively. The spectrum of **2** shows ammonium ion association (1612) and protonation (1595) as well as the fragments at 1503, the base peak corresponding to loss of a tolyl group, and at 1487, corresponding to loss of a bromide and a carbonyl group. Infrared spectra of **1** and **2** indicate facial



Scheme 1. Preparation of  $\{\mu\text{-}1,3,5\text{-}[\text{CH}(\text{pz})_2]_3\text{C}_6\text{H}_3\}[\text{Re}(\text{CO})_3\text{Br}][\text{Pt}(p\text{-tolyl})_2]_2$  (**1**) and  $\{\mu\text{-}1,3,5\text{-}[\text{CH}(\text{pz})_2]_3\text{C}_6\text{H}_3\}[\text{Re}(\text{CO})_3\text{Br}]_2[\text{Pt}(p\text{-tolyl})_2]$  (**2**).

coordination of the carbonyl groups coordinated to the rhenium atoms.

### 3.2. Solid state structures

An ORTEP representation of the heterometallic complex  $\{\mu\text{-}1,3,5\text{-}[\text{CH}(\text{pz})_2]_3\text{C}_6\text{H}_3\}[\text{Re}(\text{CO})_3\text{Br}][\text{Pt}(p\text{-tolyl})_2]_2$  (**1**) is shown in Fig. 1, and selected bond distances and angles are given in Table 2. One of the tolyl groups attached to a platinum center is disordered over two orientations in the crystal, but only one orientation is shown in the figure. The complex molecule adopts a conformation in which the two  $\text{Pt}(p\text{-tolyl})_2$  groups are oriented on opposite sides of the arene rings with the rhenium group oriented on roughly the same side of the arene linker as one of the platinum groups. As observed in similar rhenium carbonyl complexes [1,7], a carbonyl ligand (C(73)–O(73)) in **1** is oriented above the arene-linker indicating intramolecular  $\pi_{\text{CO}}\text{-}\pi_{\text{Ar}}$  interactions. The shortest (perpendicular) distance between the CO bond centroid and the arene ring plane is 2.897(7) Å while the distance between the CO bond centroid and the arene ring centroid is 3.639(7) Å. These distances reflect relatively strong  $\pi_{\text{CO}}\text{-}\pi_{\text{Ar}}$  interactions [12].

Analysis of the extended structure of **1** is hindered by disorder, but two important features can be identified. First, a 2.39 Å CH–Br interaction [13] joins adjacent complex molecules into dimeric units throughout the crystalline structure as shown in Fig. 2; and second, these dimeric units form layers of complex molecules that stack along the *b*-axis with layers of the extensively disordered solvent region in an alternating fashion comparable to

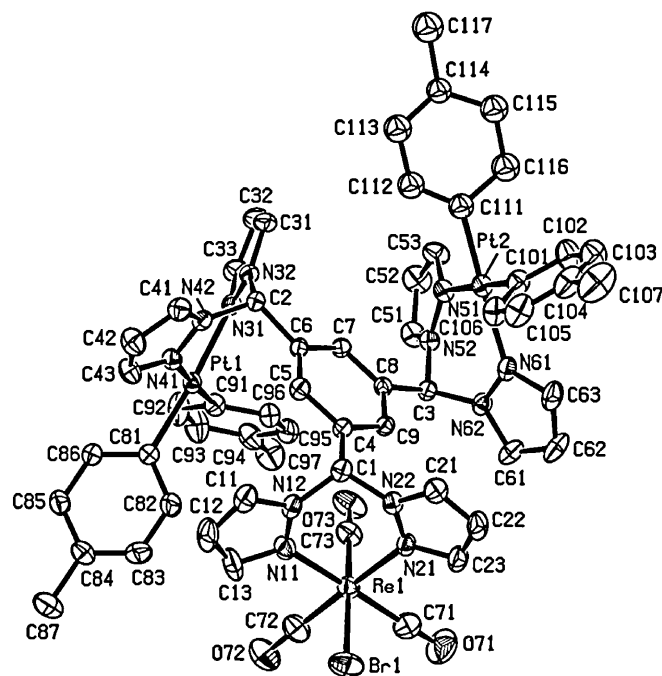


Fig. 1. ORTEP representation of  $\{\mu\text{-}1,3,5\text{-}[\text{CH}(\text{pz})_2]_3\text{C}_6\text{H}_3\}[\text{Re}(\text{CO})_3\text{Br}][\text{Pt}(p\text{-tolyl})_2]_2$  (**1**). Displacement ellipsoids are drawn at the 20% probability level. Only one component of the C(111)–C(117)/C(211)–C(217) disordered group is shown. Hydrogen atoms are omitted for clarity.

the stacking found in the previously reported homometallic rhenium complexes of this ligand [7]. Additional intralayer noncovalent interactions among the dimeric units are not observed so it is likely that solvent molecules assist in



Table 2  
Selected bond distances (Å) and angles (°) for  $\{\mu\text{-}1,3,5\text{-}[\text{CH}(\text{pz})_2]_3\text{C}_6\text{H}_3\}\text{-}[\text{Re}(\text{CO})_3\text{Br}][\text{Pt}(p\text{-tolyl})_2]_2$  (**1**)

Re(1)–C(71)	1.904(9)
Re(1)–C(72)	1.877(9)
Re(1)–C(73)	1.890(7)
Re(1)–N(11)	2.155(5)
Re(1)–N(21)	2.180(5)
Re(1)–Br(1)	2.6168(8)
Pt(1)–C(81)	2.004(5)
Pt(1)–C(91)	1.997(6)
Pt(1)–N(31)	2.099(4)
Pt(1)–N(41)	2.114(4)
Pt(2)–C(101)	2.011(5)
Pt(2)–C(111)	1.967(6)
Pt(2)–N(51)	2.113(4)
Pt(2)–N(61)	2.088(5)
C(71)–Re(1)–N(11)	174.7(3)
C(72)–Re(1)–N(11)	93.3(3)
C(72)–Re(1)–C(71)	88.9(3)
C(71)–Re(1)–Br(1)	90.8(3)
N(11)–Re(1)–Br(1)	84.42(13)
C(91)–Pt(1)–C(81)	88.6(2)
C(91)–Pt(1)–N(31)	91.4(2)
C(81)–Pt(1)–N(31)	175.25(18)
C(91)–Pt(1)–N(41)	177.5(2)
C(111)–Pt(2)–C(101)	90.8(3)
C(111)–Pt(2)–N(61)	176.2(2)
C(101)–Pt(2)–N(61)	91.1(2)
C(111)–Pt(2)–N(51)	90.2(2)

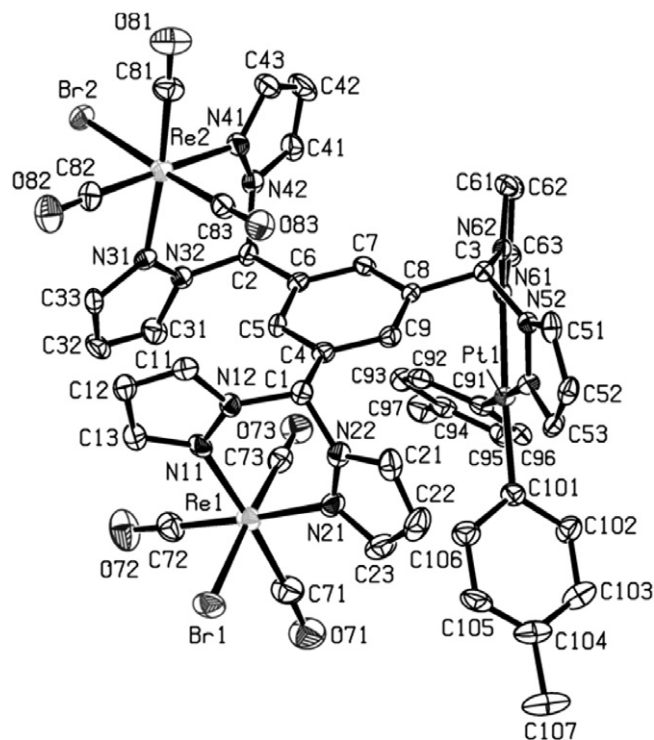


Fig. 3. ORTEP representation of the complex molecule in  $\{\mu\text{-}1,3,5\text{-}[\text{CH}(\text{pz})_2]_3\text{C}_6\text{H}_3\}[\text{Re}(\text{CO})_3\text{Br}][\text{Pt}(p\text{-tolyl})_2] \cdot \text{CH}_3\text{CN}$  ( $2 \cdot \text{CH}_3\text{CN}$ ). Displacement ellipsoids are drawn at the 40% probability level. Hydrogen atoms are omitted for clarity.

listed in Table 3. The complex molecule adopts a conformation similar to **1** in which the two rhenium groups are oriented on opposite sides of the arene rings, with the platinum group oriented on roughly the same side of the arene linker as one of the rhenium groups. As for compound **1**, compound  $2 \cdot \text{CH}_3\text{CN}$  exhibits strong  $\pi_{\text{CO}}\text{-}\pi_{\text{Ar}}$  interactions on both sides of the arene ring (C(73)–O(73), C(83)–O(83)) with both rhenium groups (shortest distances: 3.028(7) and 3.135(8) Å; centroid–centroid distances: 3.413(7) and 3.599(8) Å). Noncovalent interactions create a three-dimensional extended structure for  $2 \cdot \text{CH}_3\text{CN}$ . Most dominant are CH– $\pi$ , CH–Br, and CH–O interactions involving methine and pyrazolyl groups as hydrogen atom donors. Pyrazolyl groups, along with the bromine and carbonyl oxygen atoms, also serve as hydrogen atom acceptors.

It is interesting that in both complexes the “homobimetallic” groups are oriented on opposite sides of the linking arene ring. If these orientations are driven by simple steric factors, the opposite result might have been expected. That is, if one metal center is clearly larger than the other, the complex with two of the larger metal units would be opposite while the one with the two smaller metal centers would have these smaller metal centers on the same side of the ring. In the case of **2**, the factor driving the  $[\text{Re}(\text{CO})_3\text{Br}]$  fragments to reside on opposite sides of the central arene ring is that this orientation allows two strong  $\pi_{\text{CO}}\text{-}\pi_{\text{Ar}}$  interactions. The fact that the two  $[\text{Pt}(p\text{-tolyl})]$  groups in **1** are on opposite sides possibly implies they are the larger group, but the difference is likely small.

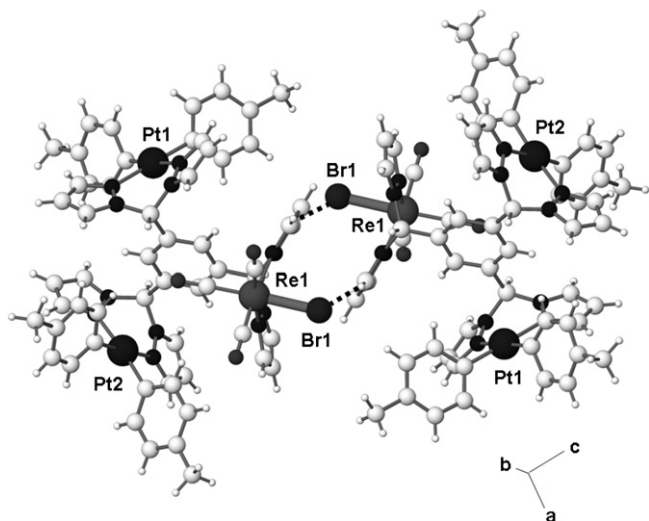


Fig. 2. Illustration of dimeric association of complex molecules in **1** created by weak, CH–Br hydrogen bonds (dashed lines). Only one component of the tolyl group disorder is shown.

organizing these layers. The disorder in the solvent region, however, prevents the identification of these interactions.

The structure of  $\{\mu\text{-}1,3,5\text{-}[\text{CH}(\text{pz})_2]_3\text{C}_6\text{H}_3\}\text{-}[\text{Re}(\text{CO})_3\text{Br}][\text{Pt}(p\text{-tolyl})_2] \cdot \text{CH}_3\text{CN}$  ( $2 \cdot \text{CH}_3\text{CN}$ ) is shown by the ORTEP drawing in Fig. 3. The asymmetric unit of the crystal contains a disordered molecule of acetonitrile. The metal complex in  $2 \cdot \text{CH}_3\text{CN}$ , however, is fully ordered. Selected bond angles and distances for  $2 \cdot \text{CH}_3\text{CN}$  are

Table 3

Selected bond distances (Å) and angles (°) for  $\{\mu\text{-}1,3,5\text{-}[\text{CH}(\text{pz})_2]_3\text{C}_6\text{H}_3\}\text{-}[\text{Re}(\text{CO})_3\text{Br}]_2[\text{Pt}(p\text{-tolyl})_2] \cdot \text{CH}_3\text{CN}$  (**2** ·  $\text{CH}_3\text{CN}$ )

Re(1)–C(71)	1.921(9)
Re(1)–C(72)	1.900(9)
Re(1)–C(73)	1.914(9)
Re(1)–N(11)	2.175(7)
Re(1)–N(21)	2.180(7)
Re(1)–Br(1)	2.6189(9)
Re(2)–C(81)	1.907(9)
Re(2)–C(82)	1.939(9)
Re(2)–C(83)	1.904(8)
Re(2)–N(31)	2.182(7)
Re(2)–N(41)	2.182(7)
Re(2)–Br(2)	2.6398(8)
Pt(1)–C(91)	1.989(7)
Pt(1)–C(101)	1.991(8)
Pt(1)–N(51)	2.105(6)
Pt(1)–N(61)	2.105(6)
C(71)–Re(1)–N(11)	174.2(3)
C(72)–Re(1)–N(11)	90.7(3)
N(11)–Re(1)–N(21)	84.1(2)
C(71)–Re(1)–Br(1)	89.2(3)
C(81)–Re(2)–N(31)	174.4(3)
C(82)–Re(2)–N(31)	90.6(3)
N(31)–Re(2)–N(41)	86.0(2)
N(31)–Re(2)–Br(2)	82.18(15)
C(91)–Pt(1)–C(101)	91.5(3)
C(91)–Pt(1)–N(61)	89.3(3)
N(51)–Pt(1)–N(61)	89.3(2)
C(91)–Pt(1)–N(51)	178.5(3)

### 3.3. Summary

The heterometallic compounds **1** and **2** have been prepared by the reaction of stoichiometric amounts of  $[\text{Pt}(p\text{-tolyl})_2(\mu\text{-SEt}_2)]_2$  with the homometallic rhenium carbonyl complexes  $\{\mu\text{-}1,3,5\text{-}[\text{CH}(\text{pz})_2]_3\text{C}_6\text{H}_3\}\text{Re}(\text{CO})_3\text{Br}$  and  $\{\mu\text{-}1,3,5\text{-}[\text{CH}(\text{pz})_2]_3\text{C}_6\text{H}_3\}[\text{Re}(\text{CO})_3\text{Br}]_2$ , respectively. These compounds demonstrate that heterometallic species may be prepared by sequential incorporation of different metal centers using the arene-linked, third-generation bis(pyrazolyl)methane ligands we have developed [1,7]. Intramolecular  $\pi_{\text{CO}}\text{-}\pi_{\text{Ar}}$  stacking appears to be an important force driving the observed structural arrangements.

### Acknowledgements

We thank the National Science Foundation (CHE-0715559) for financial support. We also thank the Alfred P. Sloan Foundation for support of R.P.W.

### Appendix A. Supplementary material

CCDC 654353 and 654354 contain the supplementary crystallographic data for **1** and **2** ·  $\text{CH}_3\text{CN}$ . These data can be obtained free of charge via <http://www.ccdc.cam.ac.uk/conts/retrieving.html> or from the Cambridge Crystallographic Data Centre, 12 Union Road, Cambridge CB2 1EZ, UK; fax: (+44) 1223-336-033; or e-mail: [deposit@](mailto:deposit@)

[ccdc.cam.ac.uk](http://ccdc.cam.ac.uk). Supplementary data associated with this article can be found, in the online version, at [doi:10.1016/j.jorganchem.2007.08.029](https://doi.org/10.1016/j.jorganchem.2007.08.029).

### References

- [1] D.L. Reger, R.P. Watson, M.D. Smith, P.J. Pellechia, *Organometallics* 24 (2005) 1544.
- [2] (a) S. Trofimenko, *Scorpionates: The Coordination Chemistry of Polypyrazolylborate Ligands*, Imperial College, London, 1999; (b) D. White, J.W. Faller, *J. Am. Chem. Soc.* 104 (1982) 1548; (c) D.L. Reger, J.R. Gardinier, W.R. Gemmill, M.D. Smith, A.M. Shahin, G.J. Long, L. Rebbouh, F. Grandjean, *J. Am. Chem. Soc.* 127 (2005) 2303; (d) D.L. Reger, J.R. Gardinier, S. Bakbak, R.F. Semeniuc, U.H.F. Bunz, M.D. Smith, *New J. Chem.* 29 (2005) 1035; (e) C.P. Brock, M.K. Das, R.P. Minton, K. Niedenzu, *J. Am. Chem. Soc.* 110 (1988) 817; (f) C. Janiak, L. Braun, F. Girgsdies, *J. Chem. Soc., Dalton Trans.* (1999) 3133; (g) J.L. Kisko, T. Hascall, C. Kimblin, G. Parkin, *J. Chem. Soc., Dalton Trans.* (1999) 1929; (h) N.C. Hardin, J.C. Jeffrey, J.A. McCleverty, L.H. Rees, M.A. Ward, *New J. Chem.* 22 (1998) 661; (i) K. Niedenzu, S. Trofimenko, *Inorg. Chem.* (1985) 4222; (j) F. Jäkle, K. Polborn, M. Wagner, *Chem. Ber.* 129 (1996) 603; (k) F. Fabrizi de Biani, F. Jäkle, M. Spiegler, M. Wagner, P. Zanello, *Inorg. Chem.* 36 (1997) 2103; (l) E. Herdtweck, F. Peters, W. Scherer, M. Wagner, *Polyhedron* 17 (1998) 1149; (m) S.L. Guo, F. Peters, F. Fabrizi de Biani, J.W. Bats, E. Herdtweck, P. Zanello, M. Wagner, *Inorg. Chem.* 40 (2001) 4928; (n) S.L. Guo, J.W. Bats, M. Bolte, M. Wagner, *J. Chem. Soc., Dalton Trans.* (2001) 3572; (o) S. Bieller, F. Zhang, F.M. Bolte, J.W. Bats, H.-W. Lerner, M. Wagner, *Organometallics* 23 (2004) 2107.
- [3] (a) V. Balzani, A. Juris, M. Venturi, S. Campagna, S. Serroni, *Chem. Rev.* 96 (1996) 759; (b) S.H.-F. Chong, S.C.-F. Lam, V.W.-W. Yam, N. Zhu, K.-K. Cheung, S. Fathallah, K. Costuas, J.-F. Halet, *Organometallics* 23 (2004) 4924; (c) J. Masllorens, A. Roglans, M. Moreno-Mañas, T. Parella, *Organometallics* 23 (2004) 2533.
- [4] (a) A. Cecon, S. Santi, L. Orian, A. Bisello, *Coord. Chem. Rev.* 248 (2004) 683; (b) J.R. Fulton, T.A. Hanna, R.G. Bergman, *Organometallics* 19 (2000) 602; (c) A. Fukuoka, S. Fukagawa, M. Hirano, N. Koga, S. Komiyama, *Organometallics* 20 (2001) 2065; (d) S. Fabre, B. Findeis, D.J.M. Trösch, L.H. Gade, I.J. Scowen, M. McPartlin, *Chem. Commun.* (1999) 577; (e) M. Schubart, G. Mitchell, L.H. Gade, T. Kottke, I.J. Scowen, M. McPartlin, *Chem. Commun.* (1999) 233; (f) A. Scheider, L.H. Gade, M. Breuning, G. Bringman, I.J. Scowen, M. McPartlin, *Organometallics* 17 (1998) 1642; (g) R.D. Adams, F.A. Cotton (Eds.), *Catalysis by Di- and Polynuclear Metal Cluster Complexes*, Wiley-VCH, New York, 1998, and references therein; (h) B.M. Trost, T. Mino, *J. Am. Chem. Soc.* 125 (2003) 2410; (i) E.N. Jacobsen, *Acc. Chem. Res.* 33 (2000) 421; (j) P. Molenveld, J.F.J. Engbersen, D.N. Reinhoudt, *Chem. Soc. Rev.* 29 (2000) 75; (k) M. Sawamura, M. Sudoh, Y. Ito, *J. Am. Chem. Soc.* 118 (1996) 3309; (l) M.E. Broussard, B. Juma, S.G. Train, W.-J. Peng, S.A. Laneman, G.G. Stanley, *Science* 260 (1993) 1784; (m) N. Guo, L. Li, T.J. Marks, *J. Am. Chem. Soc.* 126 (2004) 6542;

- (n) H. Li, L. Li, T.J. Marks, L. Liabe-Sands, A.L. Rheingold, J. Am. Chem. Soc. 125 (2003) 10788;
- (o) L. Li, M.V. Metz, H. Li, M.-C. Chen, T.J. Marks, L. Liabe-Sands, A.L. Rheingold, J. Am. Chem. Soc. 124 (2002) 12725;
- (p) J. Wang, H. Li, N. Guo, L. Li, C.L. Stern, T.J. Marks, Organometallics 23 (2004) 5112;
- (q) G.P. Abramo, L. Li, T.J. Marks, J. Am. Chem. Soc. 124 (2002) 13966.
- [5] D.L. Reger, R.F. Semeniuc, M.D. Smith, Inorg. Chem. 42 (2003) 8137.
- [6] D.L. Reger, J.R. Gardinier, M.D. Smith, Polyhedron 23 (2004) 291.
- [7] D.L. Reger, R.P. Watson, M.D. Smith, P.J. Pellechia, Organometallics 25 (2006) 743.
- [8] M.A. Casado Lacabra, A.J. Canty, M. Lutz, J. Patel, A.L. Spek, H. Sun, G. van Koten, Inorg. Chim. Acta 327 (2002) 15.
- [9] SMART Version 5.630, SAINT+ Version 6.45 and SADABS Version 2.10. Bruker Analytical X-ray Systems Inc., Madison, Wisconsin, USA, 2003.
- [10] G.M. Sheldrick, SHELXTL Version 6.1; Bruker Analytical X-ray Systems Inc., Madison, Wisconsin, USA, 2000.
- [11] PLATON, A Multipurpose Crystallographic Tool, Utrecht University, Utrecht, The Netherlands, Spek, A.L., 1998.
- [12] C. Janiak, J. Chem. Soc., Dalton Trans. (2000) 3885.
- [13] For a useful compilation of references concerning a variety of noncovalent interactions, see D.L. Reger, R.F. Semeniuc, V. Rassolov, M.D. Smith, Inorg. Chem. 43 (2004) 537.